Acta Ophthalmologica

Topographic analysis of eyelid position using digital image processing software

Yeoun Sook Chun,[1] Hong Hyun Park,[1] In Ki Park,[2] Nam Ju Moon,[1] Sang Joon Park[3,4] and Jeong Kyu Lee[1]

[1]Department of Ophthalmology, Chung-Ang University College of Medicine, Chung-Ang University Hospital, Seoul, Korea
[2]Department of Ophthalmology, Kyung Hee University College of Medicine, Kyung Hee University Hospital, Seoul, Korea
[3]Department of Radiology, Seoul National University College of Medicine, Seoul, Korea
[4]Biomedical Research Institute, Seoul National University Hospital, Seoul, Korea

ABSTRACT.

Purpose: **To propose a novel analysis technique for objective quantification of topographic eyelid position with an algorithmatically calculated scheme and to determine its feasibility.**

Methods: **One hundred normal eyelids from 100 patients were segmented using a graph cut algorithm, and 11 shape features of eyelids were semi-automatically quantified using in-house software. To evaluate the intra- and inter-examiner reliability of this software, intra-class correlation coefficients (ICCs) were used. To evaluate the diagnostic value of this scheme, the correlations between semi-automatic and manual measurements of margin reflex distance 1 (MRD1) and margin reflex distance 2 (MRD2) were analysed using a Bland–Altman analysis. To determine the degree of agreement according to manual MRD length, the relationship between the variance of semi-automatic measurements and the manual measurements was evaluated using linear regression.**

Results: **Intra- and inter-examiner reliability were excellent, with ICCs ranging from 0.913 to 0.980 in 11 shape features including MRD1, MRD2, palpebral fissure, lid perimeter, upper and lower lid lengths, roundness, total area, and medial, central, and lateral areas. The correlations between semi-automatic and manual MRDs were also excellent, with better correlation in MRD1 than in MRD2 (R = 0.893 and 0.823, respectively). In addition, significant positive relationships were observed between the variance and the length of MRD1 and 2; the longer the MRD length, the more the variance.**

Conclusion: **The proposed novel optimized integrative scheme, which is shown to have high repeatability and reproducibility, is useful for topographic analysis of eyelid position.**

Key words: digital image analysis – eyelid – repeatability – reproducibility

Acta Ophthalmol. 2017: 95: e625–e632

doi: 10.1111/aos.13437

Introduction

Objective assessment of eyelid position is essential for the diagnosis of disease, medical recording, identification of therapeutic effects, and communication in multicentre research interventions. Eyelid position is important not only in the oculoplastic field such as lid trauma, tumour, ptosis, lid retraction, or exophthalmos in Graves' ophthalmopathy, but also in the vertical ocular muscle surgery in the strabismus, exposure keratitis, and filamentary keratitis in external ocular disease, and long-term application of anti-glaucoma medication such as prostaglandin.

Currently, the subjective clinical evaluation of eyelid position is limited to linear measurements, including MRD1 (the vertical distance between the light reflex of the cornea to the centre of the upper eyelid margin), MRD2 (the vertical distance between the light reflex to the centre of the lower eyelid margin), palpebral fissure (the vertical height between the eyelids), and levator function (the extent of eyelid movement on maximum down and up gazes, while blocking the effects of the forehead; Putterman 2012). These manual measurements have definite learning curve effects, as well as weak repeatability and reproducibility (Boboridis et al. 2001). Furthermore, eyelid position and configuration cannot be described with linear measurements only, because lid contours have various features such as lid peaking and notches, lateral lid flare and scleral show, eyelid slant, entropion, and ectropion.

Accordingly, much recent research has investigated the criteria for objective assessment of the expression of eyelid position involving not only linear measurements (Edwards et al. 2004; Coombes et al. 2007; Taban et al. 2008; Zoumalan et al. 2010; Flynn et al. 2011; Kim 2013; Nishihira

et al. 2014), but also lid contours or specific parameters (Cruz et al. 1998, 2003; Chang et al. 2004; Schellini et al. 2006; Milbratz et al. 2012; Bravo et al. 2013; Mocan et al. 2014). However, most of these studies report virtual measurements instead of actual measurements, assuming arbitrary corneal diameters such as reference pixel widths (Cruz et al. 1998; Chang et al. 2004; Schellini et al. 2006; Coombes et al. 2007; Taban et al. 2008; Zoumalan et al. 2010; Flynn et al. 2011; Bravo et al. 2013; Kim 2013; Mocan et al. 2014; Nishihira et al. 2014) or a ratio to each corneal diameter (Kim 2013; Mocan et al. 2014; Nishihira et al. 2014). Also, the existing research utilizes easily accessible open programs such as ADOBE PHOTOSHOP (Adobe Systems Inc., San Jose, CA, USA; Bravo et al. 2013; Zoumalan et al. 2010) or NIH IMAGEJ software (National Institutes of Health, Bethesda, MD, USA; Chang et al. 2004; Cruz et al. 1998, 2003; Schellini et al. 2006; Taban et al. 2008; Zoumalan et al. 2010) for image analysis. Originally, those tools were developed as generally applicable programs for various kinds of image manipulation. Therefore, the programs require multiple steps and clicks for application in the ophthalmic field without mitigating the possibility of restriction for representation of ophthalmic features. In addition, some previous studies express lid contour using polynomial interpolation, but the mathematical equations are not able to determine the real features of lid contour in clinical situations (Cruz et al. 1998; Mocan et al. 2014).

Thus an optimized integrative scheme for computing eyelid topologic features with reproducible procedures in routine clinical settings is required. This study develops a dedicated analytic scheme for objective quantification of eyelids with only a few clicks within a short period of time. After defining eyelid margins with a semi-automated technique, the features of eyelids and corneas are automatically segmented by a graph cut algorithm, which enables globally optimal segmentation through the balancing of boundary and region properties (Boykov & Jolly 2001; Boykov & Kolmogorov 2004; Boykov & Funka 2006). Subsequently, 11 shape features including MRD1, MRD2, palpebral fissure, lid perimeter, upper and lower lid lengths, total area, medial area, corneal area, lateral area, and roundness are automatically computed.

Using photographs of an eyelid, we present results showing that our novel approach for topologic quantification is feasible and reproducible for clinical application of eyelid status analysis.

Materials and Methods

This study evaluates intra-examiner and inter-examiner reliability of a novel analytic technique and compares objective measurements from imaging analysis of subjects' eyelid position with subjective manual measurements determined by clinical examiner. This retrospective study was approved by the institutional review board of Chung-Ang University Hospital, and the requirement for informed consent was waived. The image acquisition, processing, and analysis were performed according to the tenets of the Declaration of Helsinki.

Image collection and subjective measurement

We collected 100 high-quality facial photographs of normal eyelids, i.e. patients who did not have significant ptosis. In particular, ptosis patients were excluded to ensure light reflection in the photographs that we did analyse. Conditions also included fine focus photographs in order to have well-defined outlining. All the images were taken by the same examiner in a room with the same conditions. With a modified slit lamp, the subjects' heads were placed on a chin rest with forehead support to position them on a consistent plane in relation to the camera and to generate standardized images of the eyelids. Subjects were instructed to relax, and the posterior strap was not used in the interest of avoiding tension in subjects. The subjects focused on the centre of the camera lens with their eyes in the primary gaze position. As a standard reference of spatial information, a ruler was attached to the forehead support frame to calculate the physical spacing between pixels and the position of the image in space through the calibration of the pixel/millimetre ratio, because simple photographs lack pixel spacing information (Fig. 1). All photographs were taken with a 12.3-megapixel automated digital camera (Nikon D90 digital camera; Nikon, Tokyo, Japan). The aperture, shutter speed, and exposure time were based on the external lighting conditions. A camera flash was not used in order to avoid the blinking reflex in the eyes of subjects. Photographs were interfaced to a personal computer (PC) and saved as JPG files (1200 × 797 pixels, 24-bit, RGB).

An experienced ophthalmologist (J.K.L.) with 15 years of experience in an oculoplastic department measured MRD1 and MRD2 lengths with the subject gazing in the primary position. The eyes of the examiner and the subject were aligned at the same level. A vertical ruler with millimetre demarcations was placed at the lateral canthi to measure length. A clinician recorded measurements to the nearest 0.5 mm unit.

Objective analysis and computerized shape analysis

Our PC-based software, EYELID ANALYSIS SOFTWARE (EAS), was used for segmentation. Automated quantification of computerized features was implemented with a dedicated C++ language with Microsoft Foundation Classes (MFC; Microsoft, Redmond, WA, USA). The overall procedure of our analysis scheme comprised two major stages. In the first stage, eyelid and cornea segmentation were performed as preprocessing steps, and in the second stage, 11 shape features were semi-automatically computed.

Two independent ophthalmologists with more than 15 years of clinical experience and one resident with one year of experience independently delineated regions of interest (ROI) for each case. Eyelid parameters were estimated using our dedicated EAS on each monitor.

Segmentation and preprocessing steps

After loading a photograph, the examiners were instructed to click 'Ruler' and to draw a 1-cm- or 1-inch-length line over the ruler on the photograph to calculate the actual spacing value of eyelid parameters through calibration of the pixel/millimetre ratio. To set ROI, we used an interactive polygonal drawing method by clicking the left mouse button to begin and by moving the mouse along the eyelid border to

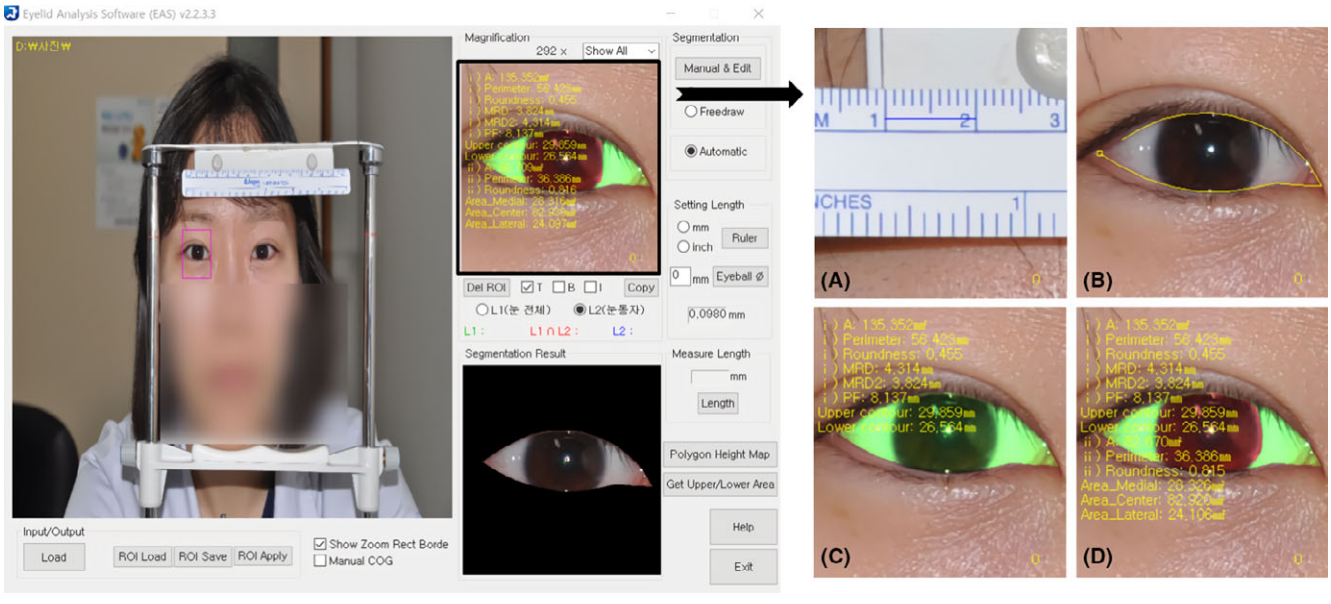

Fig. 1. Screenshot showing the EYELID ANALYSIS SOFTWARE program. (A) Drawing a 1 cm over the ruler to calculate the pixel/millimetre ratio. (B) Drawing an eyelid border using an interactive polygonal method. (C) After finishing of lining of eyelid margin, the extracted ROI was displayed with a green colour. (D) Semi-auto segmentation was conducted by clicking cornea and the cornea region was displayed in a dark pink colour. And finally, semi-automatically calculated parameters are shown on monitor.

finish with another left click at start point. When the entire outline of the eyelid was defined, the extracted ROI was displayed on the monitor with a green colour (Fig. 1).

Subsequently, the cornea region was semi-automatically extracted in a dark pink colour on the monitor (Fig. 1) using graph cut segmentation with an intensity-weighted cost function for obtaining the areas of three parts (medial, corneal, and lateral; Boykov & Funka 2006; Boykov & Jolly 2001; Boykov & Kolmogorov 2004). This graph cut algorithm was operated at the base of a statistical shape model using global optimization of a cost function including the intensity map. The basic idea of this approach is as follows.

1 Each pixel in the image is viewed as a vertex of a graph.
2 The similarity between two pixels is represented for the weight of the edge of these two vertices.
3 The segmented result is obtained by cutting edges in the graph to form a good set of connected components.

A minimum cost cut generates a segmentation that is optimal in terms of properties that are built into the edge weights. After finishing the above segmentation step, the light reflex of a subject's cornea was designated automatically by calculating the centre of mass of the eyelid and cornea regions. If the location of the light reflex point was incorrect, then the examiner manually corrected the point information.

Shape features of eyelids

After completing the segmentation step, 11 shape features were semi-automatically obtained, including MRD1, MRD2, Palpebral fissure, lid perimeter, upper and lower lid lengths, total area, medial area, corneal area, lateral area, and roundness. The MRDs were calculated as the vertical length from the light reflex of the cornea in an eyelid. Palpebral fissure was the vertical distance from the bottom of the lower eyelid margin to the top of the upper eyelid margin taken at the light reflex of the cornea, and it was the sum of the MRD1 and MRD2 (Fig. 2A). Based on both furthermost endpoints of the ROI, the upper part was designated as the upper lid length, and the lower part was designated as the lower lid length. Lid perimeter was the sum of the upper and lower lid lengths (Fig. 2B). Three areas including the areas of the medial, corneal, and lateral regions were obtained as shown in Fig. 2C. Roundness was the measure of how round an object was. Theoretically, if a targeted object is perfectly round, then the roundness value is one through isoperimetric inequality. Any particle that is not round will have a roundness value of <1, or in other words, close to zero.

Statistical analysis

To determine intra-examiner reliability, each clinician independently processed image analysis, repeating the same procedure three weeks later. Measured values were evaluated using ICCs. To determine inter-examiner reliability, measurements conducted by three different examiners were also evaluated using ICCs. intra-class correlation coefficients (ICCs) are large when there is little variation within the measurements of observers (Mocan et al. 2014).

To evaluate the diagnostic value of this scheme, the correlations between semi-automatic and manual measurements of MRD1 and MRD2 were analysed using a Bland–Altman analysis. To determine the degree of agreement according to manual MRD length, the relationship between the variance of semi-automatic measurements and the manual measurements was evaluated using linear regression.

Statistical analyses were performed using SPSS software version 19.0 (PASW, version 19.0; SPSS Inc., Chicago, IL, USA). The α level (type I error) was set at 0.05.

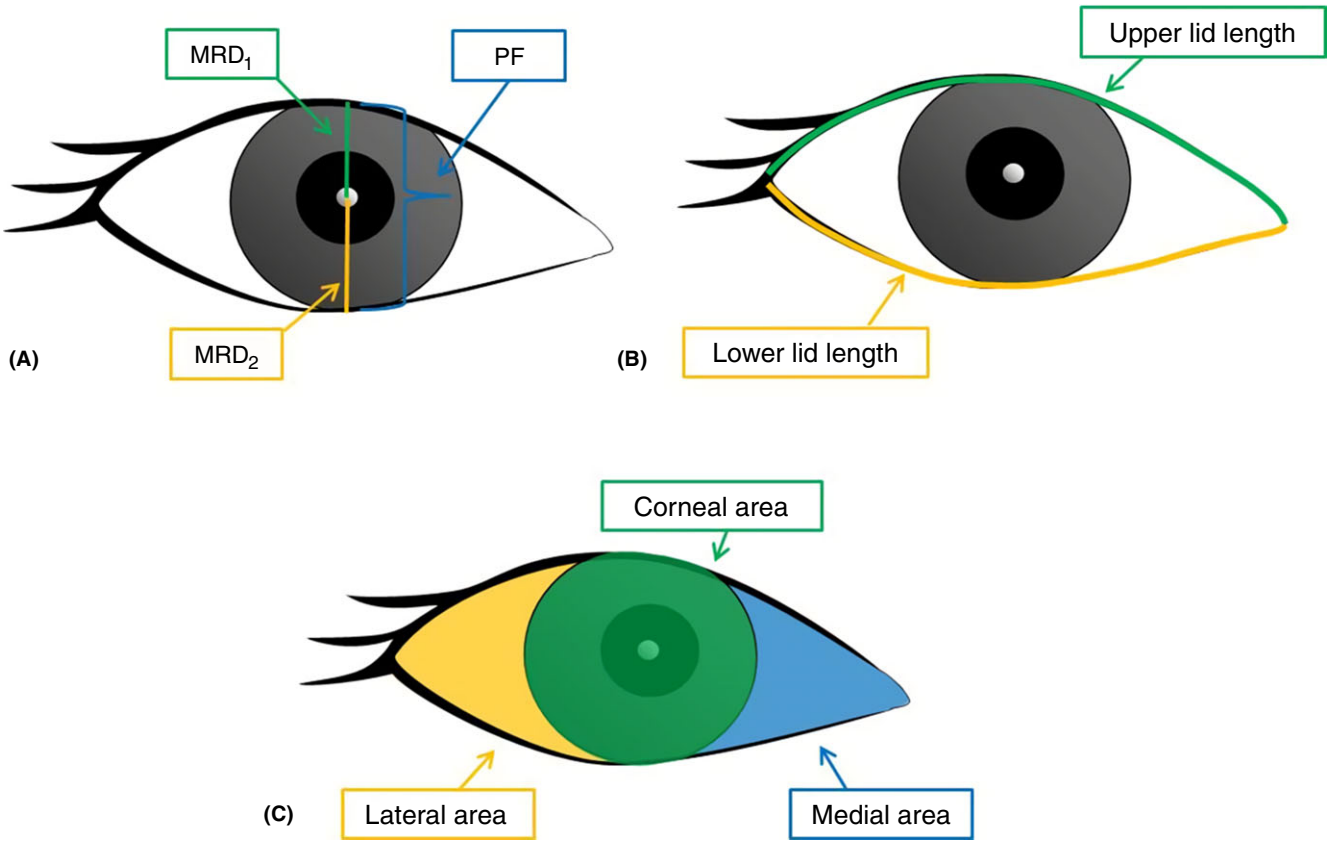

Fig. 2. (A) Vertical distance between the light reflex of the cornea to the top of the upper eyelid margin (MRD1) and to the bottom of the lower eyelid margin (MRD2). Palpebral fissure (PF) is composed of the sum of MRD1 and MRD2. (B) Lid perimeter is the total length of the sum of the upper and lower lid lengths. (C) Medial, corneal, and lateral areas within the region of interest.

Results

Three clinicians analysed 100 high-quality photographs with appropriate fixation, illumination, and fine focus. The photographs were composed of eyelids in normal eyelid positions, with different age groups, and with manual MRD1 lengths of at least 1 mm or more. The average age was 35.9 ± 13.3 years (with a range of 13–69 years), and 58 subjects were female. The characteristics of the eligible subjects for photographs are shown in Table 1.

Shape features of 100 normal eyelids

Table 2 shows values of 11 shape features in a total dataset of 600 (100 photographs × 3 examiners × 2 times). The mean MRD2 was 2.5 mm longer than the mean MRD1. Eyelid perimeter was 56.27 mm, and upper lid length was 2.9 mm (10.9%) longer than lower lid length. The total area of ROI was 144.46 mm^2, and areas of the medial and lateral regions were very similar. Corneal area occupied 54.2% within an area of ROI. The mean roundness of the eyelids was 0.47, with a range of 0.29–0.6.

Inter-examiner reliability

Inter-examiner reliability data are shown in Table 3. Reliability among the three examiners was excellent, with ICCs ranging from 0.942 to 0.980 in either or both the first and second analyses. Palpebral fissure measurements showed the best reliability (ICC = 0.977 at the first grading and 0.980 at the second grading).

Intra-examiner reliability

Intra-examiner reliability data are shown in Table 4. The repeatability between the first and second analyses was excellent among all three examiners, with ICCs ranging from 0.913 to 0.977. Lateral area measurements showed the best reliability in two of the three examiners. The resident with one year of clinical experience (examiner 3) showed the best ICC values in terms of the overall parameters, with the exception of the corneal area.

Table 1. Clinical and demographic characteristics of participants.

Subject number	100
Males:females	42:58
Age, years (mean ± SD)	35.9 ± 13.3
Age range of subjects (number)	
10–19.9	7
20–29.9	29
30–39.9	30
40–49.9	15
50–59.5	16
60–69.9	3

Agreement between subjective and objective MRD1 and MRD2 values

Subjective manual values of MRD1 and MRD2 measured by examiner 1 (J.K.L.) with a vertical ruler were compared with the objective values measured by examiner 1 using the in-house software, EAS. The mean manual MRD1 was 2.88 ± 0.89 mm, and

Table 2. Measurements of 11 shape features of normal eyelids.

	Mean ± SD	Range
MRD1 (mm)	2.87 ± 0.85	0.88–5.46
MRD2 (mm)	5.34 ± 0.81	3.42–7.57
Palpebral fissure (mm)	8.21 ± 1.24	5.12–11.09
Lid perimeter (mm)	56.28 ± 4.46	43.68–68.69
Upper lid length (mm)	29.59 ± 2.51	23.13–36.09
Lower lid length (mm)	26.69 ± 2.18	14.51–32.59
Area (mm^2)	144.46 ± 30.14	78.62–229.44
Medial area (mm^2)	33.36 ± 10.02	10.17–64.68
Corneal area (mm^2)	78.34 ± 11.92	51.21–117.12
Lateral area (mm^2)	32.22 ± 11.74	7.49–64.00
Roundness	0.47 ± 0.06	0.29–0.60

SD = standard deviation; MRD1 = margin reflex distance from the corneal light reflex to the upper eyelid margin; MRD2 = margin reflex distance from the corneal light reflex to the lower eyelid margin; Lid perimeter = upper lid length + lower lid length; Area = medial area + corneal area + lateral area in the region of interest.

Table 3. Intra-class correlation coefficients (ICCs) for inter-examiner reliability among three examiners at first and second digital imaging analyses for topographic evaluation of eyelid shape in normal eyelids.

	ICCs at the first grading (95% CI)	p-Value	ICCs at the second grading (95% CI)	p-Value
MRD1 (mm)	0.965 (0.952, 0.976)	<0.001	0.958 (0.941, 0.970)	<0.001
MRD2 (mm)	0.955 (0.937, 0.968)	<0.001	0.970 (0.959, 0.979)	<0.001
Palpebral fissure (mm)	0.977 (0.967, 0.984)	<0.001	0.980 (0.973, 0.986)	<0.001
Lid perimeter (mm)	0.952 (0.933, 0.966)	<0.001	0.962 (0.948, 0.974)	<0.001
Upper lid length (mm)	0.977 (0.968, 0.984)	<0.001	0.979 (0.970, 0.985)	<0.001
Lower lid length (mm)	0.942 (0.925, 0.962)	<0.001	0.972 (0.961, 0.980)	<0.001
Area (mm^2)	0.956 (0.939, 0.969)	<0.001	0.980 (0.973, 0.986)	<0.001
Medial area (mm^2)	0.976 (0.967, 0.983)	<0.001	0.972 (0.961, 0.980)	<0.001
Corneal area (mm^2)	0.952 (0.933, 0.966)	<0.001	0.970 (0.958, 0.979)	<0.001
Lateral area (mm^2)	0.977 (0.968, 0.984)	<0.001	0.957 (0.941, 0.970)	<0.001
Roundness	0.975 (0.966, 0.983)	<0.001	0.977 (0.969, 0.984)	<0.001

CI = confidence interval; MRD1 = margin reflex distance from the corneal light reflex to the upper eyelid margin; MRD2 = margin reflex distance from the corneal light reflex to the lower eyelid margin; Lid perimeter = upper lid length + lower lid length; Area = medial area + corneal area + lateral area in the region of interest.
p-Value by the intra-class correlation coefficients.

Table 4. Intra-class correlation coefficients (ICCs) for intra-observer reliability between the first and second measurements for topographic evaluation of normal eyelid shapes using digital imaging analysis.

	Examiner 1	Examiner 2	Examiner 3
MRD1 (mm)	0.945	0.958	0.972
MRD2 (mm)	0.930	0.937	0.957
Palpebral fissure (mm)	0.964	0.971	0.973
Lid perimeter (mm)	0.922	0.957	0.957
Upper lid length (mm)	0.949	0.938	0.951
Lower lid length (mm)	0.934	0.913	0.937
Area (mm^2)	0.934	0.972	0.973
Medial area (mm^2)	0.967	0.962	0.962
Corneal area (mm^2)	0.946	0.966	0.927
Lateral area (mm^2)	0.964	0.975	0.982
Roundness	0.968	0.965	0.977

MRD1 = margin reflex distance from the corneal light reflex to the upper eyelid margin; MRD2 = margin reflex distance from the corneal light reflex to the lower eyelid margin; Lid perimeter = upper lid length + lower lid length; Area = medial area + corneal area + lateral area in the region of interest.
p-Value is <0.001 for all data by the intra-class correlation coefficients.

the mean objective MRD1 was 2.89 ± 0.86 mm. There was no significant difference between the mean manual and objective values of MRD1 (Student *t*-test, p = 0.40). The mean manual MRD2 was 5.21 ± 0.64 mmn and the mean objective MRD2 was 5.33 ± 0.82 mm. The value of the objective MRD2 was larger than that of the manual MRD2 (Student *t*-test, p = 0.006).

Bland–Altman plots also confirmed excellent reliability and showed acceptable limits of agreement for MRD1 and 2 (Fig. 3B and D). The correlation in MRD1 was better than that in MRD2.

The variance according to the length of manual MRD was evaluated. There was a significant positive correlation between the variance and the length of MRD1 ($y = 0.843x + 0.535$; $R^2 = 0.79$; $p < 0.001$) and of MRD2 ($y = 1.053x - 0.155$; $R^2 = 0.677$; $p < 0.001$). This means that the variance increased with MRD1 length. While the variance also increased with MRD2 length, the variance was largest in the manual MRD2 length of 5 mm (Fig. 3).

Discussion

This study proposed a novel optimized integrative technique for topologic quantification of eyelid position using dedicated in-house software. Our techniques showed excellent intra-examiner and inter-examiner reliability, and the correlations between subjective manual and objective measurements were excellent in both MRD1 and MRD2. The correlation in MRD1 was better than the correlation in MRD2.

In actual clinical practice, manual MRD1, MRD2, and palpebral fissure are the main parameters for evaluating eyelid position. These manual measurements are influenced by the experience of clinicians on the learning curve effect and are dependent on the intuitive observations of clinicians (Boboridis et al. 2001). The study of Boboridis et al. (2001) reports that there is a mean difference of up to 0.5 mm on MRD according to the level of clinician experience. Therefore, variance in manual assessment is natural. In this study, the correlation between semi-automatic and manual measurements was better in MRD1 than in MRD2, and the variance increased with MRD length. Accordingly, we are able to surmise

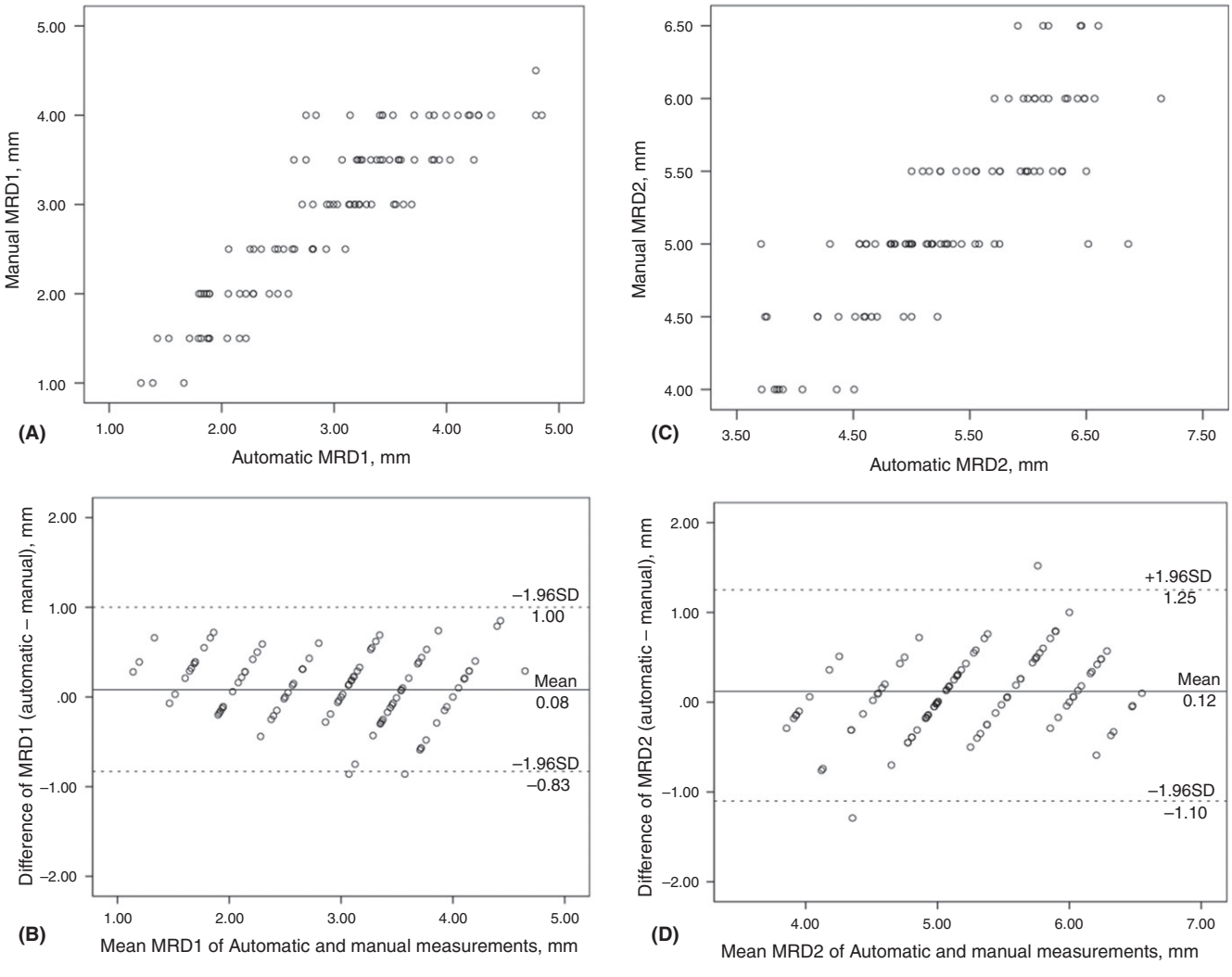

Fig. 3. (A) Scatter plot of semi-automatic and manual MRD1 measurements. There was a significant positive correlation between variance and MRD length. Variance increased with MRD1 length ($y = 0.843x + 0.535$; $R^2 = 0.79$; $p < 0.001$). (B) A Bland–Altman analysis of the MRD1 results. The correlations between semi-automatic and manual MRD1 measurements were excellent. (C) Scatter plot of semi-automatic and manual MRD2 measurements. There was a significant positive correlation between variance and MRD length. Variance increased with MRD2 length ($y = 1.053x - 0.155$; $R^2 = 0.677$; $p < 0.001$). (D) A Bland–Altman analysis of the MRD2 results. The correlations between semi-automatic and manual MRD2 measurements were excellent.

that when an examiner manually measures MRD with a vertical ruler, MRD1 is more exactly and constantly measurable than MRD2. Close attention must be paid in measuring long MRDs, because the longer the MRD, the greater the variance in measurements.

Interesting results were found in our analysis of the data. While the intra-examiner reliability data were excellent among all three examiners, the resident with one year of clinical experience showed the best ICC values in terms of the overall parameters, with the exception of the corneal area. This means that if an examiner were to meticulously conduct an ROI drawing, then the reliability of the software program would be high regardless of the examiner's level of clinical experience. This proves that our novel software for the topologic quantification of eyelid position is an accurate and easy tool for beginners or non-medical persons to work with medical images. This finding directly opposes the idea that manual measurements are influenced by a clinician's level of experience (Boboridis et al. 2001).

Objective measurements of MRDs were larger than manual measurements of MRDs and the variance was larger in MRD2 than in MRD1 in our results. These findings are similar to the work of Bodnar et al. (2016), although the authors took all photos with a camera flash and they used Canny edge detection method (Canny 1986) for comprising parameter tuning. The preprocessing step of segmentation procedures is very important to ensure accurate repeatable and reproducible imaging parameters. Canny edge detection (Canny 1986) is a useful algorithm for the detection of structural alterations with intense contrasts or with sharp margins. In ophthalmic imaging, however, the method may reduce accuracy because results are sensitive to the low-contrast intensity around adjacent structures in the eyelids, particularly for RGB colour images. Instead, we use a graph cut algorithm (Boykov & Jolly 2001; Boykov & Kolmogorov 2004; Boykov & Funka 2006), which provides globally optimal segmentation when the cost function is defined. Graph cut algorithms minimize energy functions composed of data terms that

reflect how each pixel fits into prior information and smoothness terms that penalize discontinuities between neighbouring pixels. Therefore, graph cut algorithms have been applied to medical imaging processing in various areas (Alba et al. 2014; McClymont et al. 2014; Platero & Tobar 2014).

Determination of the vertical heights of MRD1, MRD2, and palpebral fissure is a simple conventional measurement tool. These measures, however, do not provide sufficient information about various lid shapes, such as lid peaking and notches, lid flare and scleral show, lid slant, and other features. Accordingly, several studies have tried various measurement tools, with useful results (Cruz et al. 1998, 2003; Chang et al. 2004; Schellini et al. 2006; Milbratz et al. 2012; Bravo et al. 2013; Mocan et al. 2014). The approaches to image analysis in these previous studies, however, are not integrative and therefore yield results that are partial and fragmentary. In this study, we proposed novel software with an integrative approach that includes both conventional eyelid measurement and specially designed lid shape measurement with a few clicks.

To the best of our knowledge, the concept of eyelid perimeter and roundness is introduced for the first time in this study. It is intuitively understood that upper eyelid length is considerably longer than lower lid length. Until now, however, there has been no empirical information about this common observation. With our novel approach, we determined that the difference between upper and lower lid length is 2.9 mm in the normal eyelids of Asians. A racial comparison of eyelid length would be interesting, because Asian eyes have an upward lower lid slant relative to other races with lower lid slants that are comparatively flat. Roundness values were introduced herein to objectively present lid contour abnormalities. Eyelids are ovoid features rather than round ones. According to our findings, the mean roundness of eyelids was 0.47, with a range of 0.29–0.6 in the normal eyelids of Asians. Among 10 feature parameters, palpebral fissure showed the best correlation with roundness ($R = 0.776$, $p < 0.001$ by Pearson's correlation). This means that eyes with longer palpebral fissures have eyelids that are rounder in shape. Therefore, eyes with longer palpebral fissures such as lid retraction or exophthalmos in Graves' ophthalmopathy would have more round feature. The change in roundness after correction of dermatochalasis would be useful shape index for the evaluation of the eyelid contour change after surgery.

The corneal area occupied 54.2% within the total area of eyelids, and the medial and lateral regions showed similar areas to one another. Through information about the areas of these three regions, we are able to intuitively form an idea of the characteristics of eyelid configuration. Therefore, it would be valuable for future research to compare changes in lid length, area, and roundness following surgery for Graves' ophthalmopathy.

One strong point of this study is that the dedicated in-house software is shown to be very feasible for actual clinical situations because the average performance time of the entire procedure of loading a single image on the interface to producing 11 objective parameters occurs within 30 seconds. In addition, this software provides optimized integrative information regarding not only conventional eyelid measurements, but also eyelid configurations such as lid perimeter, ocular area, and roundness. Another strong point is that the digital image analysis herein shows excellent reliability regardless of the level of clinical experience of examiners. Therefore, the digital imaging provides an objective and reproducible assessment of eyelid position. A third strong point is that we calculate the actual values of eyelid position through a ruler attached to the slit lamp, which is different from other studies that use reference pixel width or ratio. A final strength of this study is in consistently controlling the head position and movement of subjects using a modified slit lamp. In this way, our method avoids horizontal or vertical head tilt and maintains the same plane of subjects for the camera. In order to avoid wrinkles in the eyelids of subjects, our technique does not use a camera flash.

There are some limitations in our study. The study included only subjects with normal eyelid positions because the purpose of the study is determination of the feasibility of the novel imaging software for clinical application. It would be a considerable challenge to evaluate ptosis in subjects with negative MRD1 using the proposed approach. In addition, although this study introduced 11 reliable feature parameters for the analysis of eyelid status, it is possible to designate more powerful parameters for representing eyelid topology (i.e. palpebral angle, focal lid abnormality, and relationship with eyebrows), and future studies will extend this aspect of our work.

In conclusion, we introduced a novel approach to eyelid imaging using new, dedicated software that was specially designed to evaluate topographic eyelid position. This optimized integrative scheme with high repeatability and reproducibility is shown to be useful for topographic analysis of eyelid position.

References

Alba X, Figueras IVRM, Lekadir K, Tobon-Gomez C, Hoogendoorn C & Frangi AF (2014): Automatic cardiac LV segmentation in MRI using modified graph cuts with smoothness and interslice constraints. Magn Reson Med **72**: 1775–1784.

Boboridis K, Assi A, Indar A, Bunce C & Tyers AG (2001): Repeatability and reproducibility of upper eyelid measurements. Br J Ophthalmol **85**: 99–101.

Bodnar ZM, Neimkin M & Holds JB (2016): Automated ptosis measurements from facial photographs. JAMA Ophthalmol **134**: 146–150.

Boykov Y & Funka LG (2006): Graph cuts and efficient N-D image segmentation. Int J Comput Vision **70**: 109–131.

Boykov Y & Jolly MP (2001): Interactive graph cuts for optimal boundary & region segmentation of objects in N-D images. Int Conf Comp Vis **1**: 105–112.

Boykov Y & Kolmogorov V (2004): An experimental comparison of min-cut/max-flow algorithms for energy minimization in vision. IEEE Trans Pattern Anal Mach Intell **26**: 1124–1137.

Bravo FG, Kufeke M & Pascual D (2013): Incidence of lower eyelid asymmetry: an anthropometric analysis of 204 patients. Aesthet Surg J **33**: 783–788.

Canny J (1986): A computational approach to edge detection. IEEE Trans Pattern Anal Mach Intell **8**: 679–698.

Chang EL, Bernardino CR & Rubin PA (2004): Normalization of upper eyelid height and contour after bony decompression in thyroid-related ophthalmopathy: a digital image analysis. Arch Ophthalmol **122**: 1882–1885.

Coombes AG, Sethi CS, Kirkpatrick WN, Waterhouse N, Kelly MH & Joshi N (2007): A standardized digital photography system with computerized eyelid measurement analysis. Plast Reconstr Surg **120**: 647–656.

Cruz AA, Coelho RP, Baccega A, Lucchezi MC, Souza AD & Ruiz EE (1998): Digital image processing measurement of the upper eyelid contour in Graves disease and congenital blepharoptosis. Ophthalmology **105**: 913–918.

Cruz AA, Akaishi PM & Coelho RP (2003): Quantitative comparison between upper eyelid retraction induced voluntarily and by Graves orbitopathy. Ophthal Plast Reconstr Surg **19**: 212–215.

Edwards DT, Bartley GB, Hodge DO, Gorman CA & Bradley EA (2004): Eyelid position measurement in Graves' ophthalmopathy: reliability of a photographic technique and comparison with a clinical technique. Ophthalmology **111**: 1029–1034.

Flynn TH, Rose GE & Shah-Desai SD (2011): Digital image analysis to characterize the upper lid marginal peak after levator aponeurosis repair. Ophthal Plast Reconstr Surg **27**: 12–14.

Kim SS (2013): Effects in the upper face of far east Asians after Oriental blepharoplasty: a scientific perspective on why Oriental blepharoplasty is essential. Aesthetic Plast Surg **37**: 863–868.

McClymont D, Mehnert A, Trakic A, Kennedy D & Crozier S (2014): Fully automatic lesion segmentation in breast MRI using mean-shift and graph-cuts on a region adjacency graph. J Magn Reson Imaging **39**: 795–804.

Milbratz GH, Garcia DM, Guimaraes FC & Cruz AA (2012): Multiple radial midpupil lid distances: a simple method for lid contour analysis. Ophthalmology **119**: 625–628.

Mocan MC, Ilhan H, Gurcay H, Dikmetas O, Karabulut E, Erdener U & Irkec M (2014): The expression and comparison of healthy and ptotic upper eyelid contours using a polynomial mathematical function. Curr Eye Res **39**: 553–560.

Nishihira T, Ohjimi H & Eto A (2014): A new digital image analysis system for measuring blepharoptosis patients' upper eyelid and eyebrow positions. Ann Plast Surg **72**: 209–213.

Platero C & Tobar MC (2014): A multiatlas segmentation using graph cuts with applications to liver segmentation in CT scans. Comput Math Methods Med **2014**: 182909.

Putterman AM (2012): Margin reflex distance (MRD) 1, 2, and 3. Ophthal Plast Reconstr Surg **28**: 308–311.

Schellini SA, Sverzut EM, Hoyama E, Padovani CR & Cruz AA (2006): Palpebral dimensions in Brazilian children: assessment based on digital images. Orbit **25**: 209–213.

Taban M, Taban M & Perry JD (2008): Lower eyelid position after transconjunctival lower blepharoplasty with versus without a skin pinch. Ophtha Plast Reconstr Surg **24**: 7–9.

Zoumalan CI, Lattman J, Zoumalan RA & Rosenberg DB (2010): Orbicularis suspension flap and its effect on lower eyelid position: a digital image analysis. Arch Facial Plast Surg **12**: 24–29.

Received on July 3rd, 2016.
Accepted on February 4th, 2017.

Correspondence:
Jeong Kyu Lee, MD
Department of Ophthalmology
Chung-Ang University College of Medicine
Chung-Ang University Hospital
102 Heukseok-ro
Dongjak-gu
Seoul 156-755
Korea
Tel: +82 2 6299 1666
Fax: +82 2 6299 3231
Email: lk1246@hanmail.net
and
Sang Joon Park, PhD
Department of Radiology and Biomedical Research Institute
Seoul National University Hospital
101 Daehak-ro
Jongno-gu
Seoul, 110-744
Korea
Tel: +82 2 2072 2584
Fax: +82 2 743 6385
Email: lunao78@snu.ac.kr

Due to the characteristics of this study, an ophthalmologist and a computer scientist are co-corresponding authors.

Jeong Kyu Lee, corresponding author, has full access to all of the data in the study and takes responsibility for the integrity of the data and the accuracy of the data analysis. All authors have no conflicts of interest and Jeong Kyu Lee has financial support by the Basic Science Research Program through the National Research Foundation of Korea (NRF) funded by the Ministry of Education (NRF-2015R1D1A1A01060016).

Supporting Information

Additional Supporting Information may be found in the online version of this article:

Video S1. Demonstration of the actual operation of EYELID ANALYSIS SOFTWARE.